

ABUNUMAH, O., OGUNLUDE, P., OGOUN, E., RAMALAN, M., ANTWI, S., AISUENI, F., HASHIM, I. and GOBINA, E. 2022. Effect of reservoir structural rhythm on carbon capture and sequestration (CCS) performance. *International journal on engineering, science and technology* [online], 4(1), pages 41-53. Available from: <https://doi.org/10.46328/ijonest.72>

Effect of reservoir structural rhythm on carbon capture and sequestration (CCS) performance.

ABUNUMAH, O., OGUNLUDE, P., OGOUN, E., RAMALAN, M., ANTWI, S., AISUENI, F., HASHIM, I. and GOBINA, E.

2022

© 2022 *International Journal on Engineering, Science and Technology*.

Effect of Reservoir Structural Rhythm on Carbon Capture and Sequestration (CCS) Performance

Ofasa Abunumah

Robert Gordon University, United Kingdom

Priscilla Ogunlode

Robert Gordon University, United Kingdom

Evans Ogoun

Robert Gordon University, United Kingdom

Muktar Ramalan

Robert Gordon University, United Kingdom

Samuel Antwi

Robert Gordon University, United Kingdom

Florence Aisueni

Robert Gordon University, United Kingdom,

Idris Hashim

Robert Gordon University, United Kingdom

Edward Gobina

Robert Gordon University, United Kingdom, e.gobina@rgu.ac.uk

Abstract: In addition to the evolution of green and nano energy, sequestration of CO₂ is also an evolving method to control the global CO₂ footprint and greenhouse effect. Carbon Capture and Sequestration (CCS) is an established technique to capture carbon from anthropogenic sources, such as power and chemical plants, and then inject the same in subsurface rock micropores, to permanently store the CO₂. Besides its environmental credentials, CCS also offers economic opportunities in Gas Enhanced Oil Recovery and Methane displacement in coalbed reservoirs. CCS process incorporates various geological, geometrical and engineering understandings of porous media and fluid dynamics. Previous investigators have identified low permeability rock as a better site for CCS. However, little is known of the propagation and effectiveness of CCS in reservoirs that have multiple layers of sedimentation, vis-à-vis well topology and density, flow direction, storage site, and power optimisation. In reality, these layers altogether form a structural rhythm and gradient. In this study, we investigated the structural rhythms and gradients that optimise CCS by using two objective functions (Darcy and interstitial flowrates) and 15 structural criteria (such as pore size, porosity, tortuosity, and aspect ratio). An experimental method has been applied. Five analogous reservoir porous core samples with varying structural parameters have been tested. The results indicate that CCS optimisation is responsive to structural parameters. The rhythm analysis from this study suggests that the CCS gas flow requires a compound rhythm that has a positive porosity and negative pore gradients. That is, the CCS injection wells should be placed in the reservoir area with relatively low porosity (3%) and large pore size (6000nm), while the storage site should be at a relatively high porosity (20%) and smaller pore size (200nm). This study can be directly applied to CCS practice, such that, given a layered reservoir, engineers can predict the well placement or topology that would optimize some of the essential performance objectives of CCS.

Keywords: Carbon Capture and Sequestration, gas dynamic, CO₂, greenhouse effect, structural rhythm

Introduction

CO₂ is a very important ecosystem gas, which takes up a critical role in the carbocycle. As an example, CO₂ is a key ingredient in plant photosynthesis. However, one of the major culprits in climate change is CO₂ proliferation (Anderson William White Wallace Broecker et al., 1999; Crowley et al., 2001; den Elzen et al.,

2013; Hertzberg et al., 2017; Ledley et al., 1999; Mintzer, 1990; Shine & Sturges, 2007), which result in the so-called greenhouse effect that increases the Earth's effective temperature (global warming). The industrial revolution has been implicated in the increased generation of CO₂ and greenhouse footprint. Consequently, the effort to control climate change has been a top burner issue for the past 3 decades. There has been continued interest in the political, economic, academic and environmental spheres to resolve the incident of climate change incidental to CO₂ (IPCC, 2018; Neele et al., 2014; Samset et al., 2020). Stakeholders have suggested several solutions to mitigate the greenhouse effect of CO₂ such as the use of natural gas, solar and nuclear energy sources instead of coal or oil; reducing the deforestation rate and limiting the use of automobiles that runs on fossil fuel (Samset et al., 2020).

Besides the environmental implication of CO₂ mentioned above, CO₂ also have some economic implication. A major one is its utility in the production of trapped oil and gases from subsurface reservoirs. This process lends itself to resolving the greenhouse effect of CO₂ if the process eventually allows CO₂ to be stored or sequestered in the space vacated by the produced oil and gas. The process of using gas to produce trapped oil is called gas enhanced oil recovery (GEOR). It involves injecting CO₂ through an injection well into an oil reservoir containing oil droplets that are trapped and could not be mobilised to the production well due to capillary forces and the relatively low oil saturation. The injected gas displaces the oil droplets towards the production well through momentum or energy exchange. It is said that this process can produce 5% to 20% of the oil initially in place (OIIIP) (Andrei & de Simoni, 2010; Verma, 2015).

The mechanisms of the displacement are immiscible and miscible displacement (al Adasani & Bai, 2011; Saleh Aidrous Abdulla Al Wahedi & Eddine Dadach, 2013). Immiscible displacement is patterned like a piston-like displacement through the pores of the reservoir. While miscible displacement involves CO₂ molecule mixing with the oil droplets to form a more mobile mixture that can easily migrate through the pores of the reservoirs. In both mechanisms, some gas molecules become trapped. Investigators mentioned that 30% to 60% of the injected gases are produced along with the displaced oil (Andrei & de Simoni, 2010). The produced CO₂ can be separated from the oil and recycled for further injection. For each cycle of injection, 20% to 60% of injected gas molecules are trapped and stored (Saleh Aidrous Abdulla Al Wahedi & Eddine Dadach, 2013). This implies that in the long run, there would be a significant cumulative CO₂ gas trapped in reservoir pores. Some authors have quantitatively identified that the amount of CO₂ trapped in the lifespan of the injection process is approximately equal to the amount of CO₂ generated in the consumption of the produced oil, leading to a net-zero or neutral carbon emission for the CO₂ EOR process (McGlade Christophe, 2019; Passalacqua & Strack, 2020). Therefore, the long-term reliability and integrity of such gas trappings are of significant interest to climate change stakeholders. Because it offers an opportunity for CO₂ molecules to be captured from anthropogenic generating CO₂ sources and then sequestered in subsurface reservoirs pores that were previously occupied by oil molecules. This is popularly called Carbon Capture and Sequestration (CCS). Overall, the CCS process satisfies the mitigation of the CO₂ greenhouse effect of climate change; the economic production of oil; and the net-neutral-CO₂ utilisation of oil.

Selecting a reservoir site suitable enough to ensure the reliability and integrity of CCS outcomes is very important. The right selection should ensure technical applicability and practicality to reservoir engineers, ensure economic potential to investors, and guarantee greenhouse solution confidence to environmentalists and politicians.

On a bulk scale, geological formations are usually featured in layers (Wu & Liu, 2019). Figure 1 shows the outlook of reservoir layers. Each of these layers is a potential CCS site, and the layers could respectively possess a distinct representation of geological and geometrical parameters that would influence engineering decision making in selecting the optimal sites for CCS. Such engineering decisions include well location, well density, compression pump and power requirements, gas injection rates and oil production rates.

Furthermore, the natural arrangement of the different layers altogether leads to a structural rhythm and gradient phenomena. These phenomena consequently increase the degree of freedom and could complicate engineering decision making. Therefore, it behoves the reservoir engineers to understand how these parameters and entities can be coupled and manoeuvred to achieve CCS optimisation. Due to the nature of the deposit of sediments and geological fault, some of the layers would appear to be in parallel alignment as represented in block A in Figure 1. While a non-sealing fault can cause some layers to be connected in series as shown in block B of Figure 1. The non-sealing nature allows fluid to transmit from one layer to the next as shown in block B.

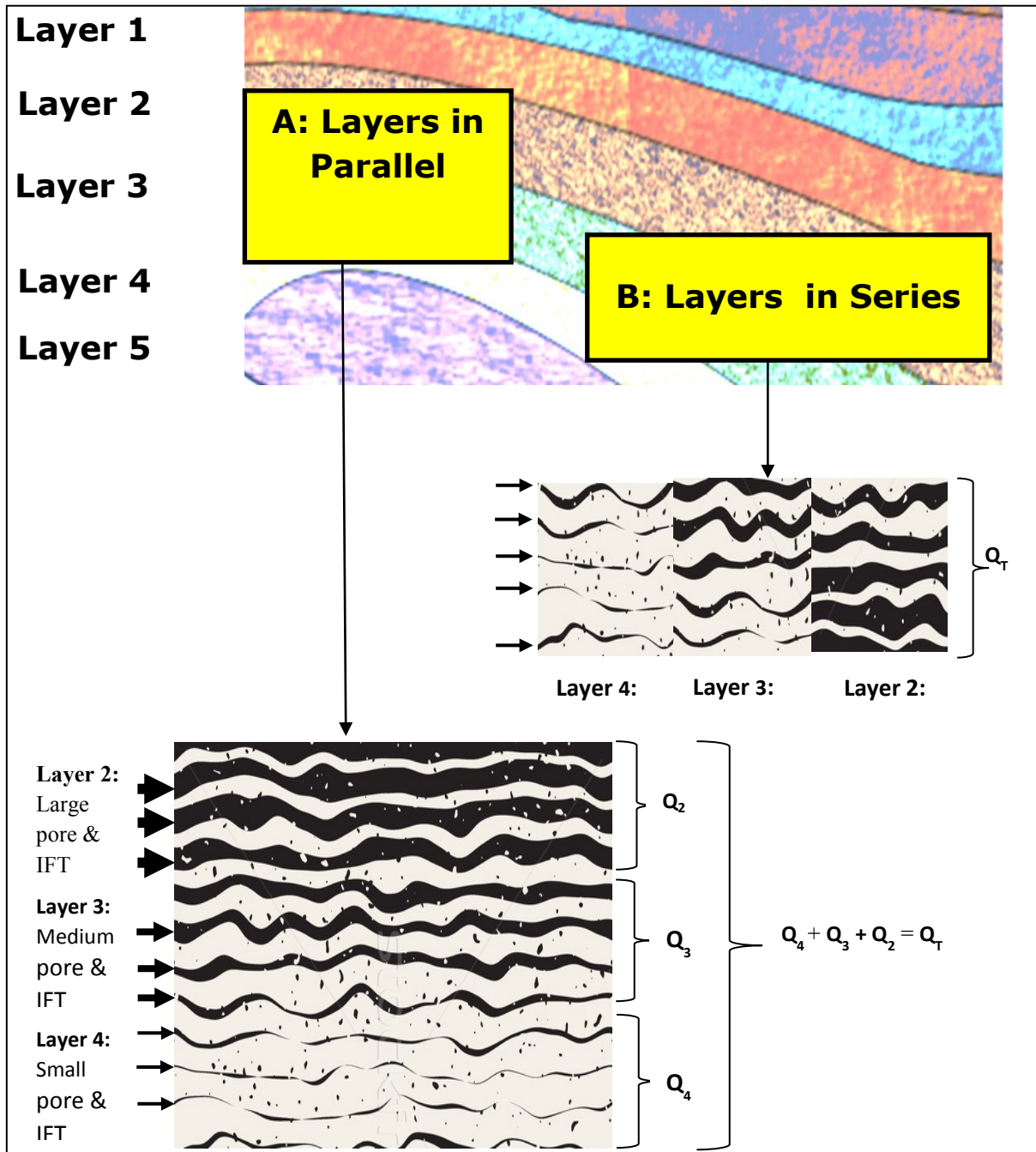


Figure 1. The Structural Laying of Geological Sediments in an Oil Reservoir

Given a porous system with three blocks of equal thickness but different pores sizes (such as $d_1=15\text{nm}$ and $d_2=200\text{nm}$, and $d_3=6000\text{nm}$) and porosity that can be hypothetically moved around, the maximum number of combinations or topologies available to optimise CCS through functions such as flow rate and mobility is 6. The 6 combinations are shown in Figure 2. Each of the topologies represents a structural rhythm. One of the study's objectives is to experimentally identify the CO_2 permeation and rhythm coupling that would optimise CS, and reduce operational complexity and technicality. Since the flow in porous media depends on the direction of flow, it is expected that the CS would respond differently to structural and geometrical gradients, such as the 6 compound pore gradients in Figure 2.

The three main elements of CCS optimisation are maximum sequestered gas quantity and high sequestration reliability and integrity. The sequestration reliability demonstrates that the gas molecules would be consistently confiscated in the pore matrixes. Such that CO_2 gas flow through or away from the site is not possible for the conditions under consideration. This method of investigating CCS has not been well published. Thus, this study has considered CCS using CO_2 Darcy and interstitial flow throughput as the objective functions. The objective

functions were subsequently coupled with the respective geological and geometrical parameters to understand how these parameters affect the propagation of CCS. The objective functions were further coupled with the structural rhythm and gradient entities.

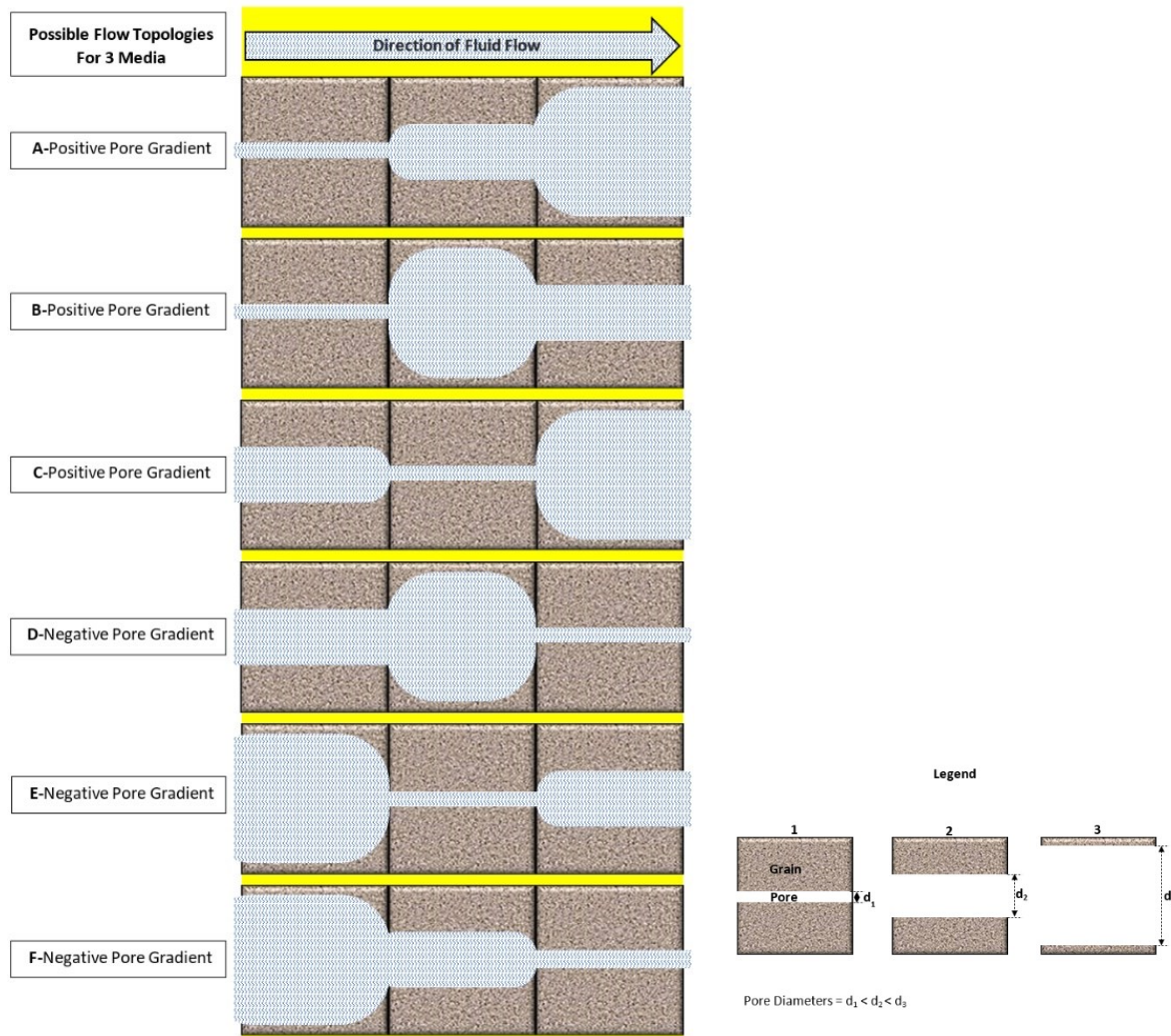


Figure 2. Potential Topologies for Optimising CO₂ EOR CS

Method

A rigorous experimental method has been applied to identify the structural characterisation of reservoir sites that are suitable for CCS. Five analogous reservoir core samples have been used. The optimisation requirement for the objective function is to minimise the Darcy and interstitial flow rates or permeation of CO₂. Therefore, a core sample that allows the least CO₂ interstitial flow rate or permeation is considered a suitable site for CCS.

Without loss of generalisation, the structural characteristics of such samples are considered to be the equivalent structural requirements of a geological CCS site at a reservoir scale. The layers alignment or rhythm and gradients that engender or facilitate the minimum order of interstitial flow rate are considered the equivalent rhythm and gradient for CSS optimisation at a reservoir scale.

Supporting Equations

The theoretical and empirical supports for describing the respective geological and engineering quantities are codified in the equations shown below. The equations also provide information on how some of the relevant structural quantities used in this study were obtained.

1. Pressure = P
2. Temperature = T
3. Gas Constant = R
4. Compressibility Factor = Z
5. Number of Moles = n
6. Volume = V
7. Core Outer Radius = r_{outer}
8. Core Inner Radius = r_{inner}
9. Pore Size, r_{pore} = Supplied by manufacturer
10. Porosity, $\phi = 1 - \left(\frac{\text{Specific Particle Density}}{\text{Specific Bulk Density}} \right)$
11. Tortuosity, $\tau = (1 - 0.41 \ln \phi)$
12. Pay Zone or Core Height, h
13. Gas Entering Surface Area, $A = 2\pi r_{outer} h$
14. Pore/Radial Thickness, $r_{thickness} = r_{outer} - r_{inner}$
15. Aspect Ratio, $AR = \frac{r_{pore}}{r_{thickness}}$
16. Gradient, $\lambda = \left(\frac{\text{entity value}_{CS \text{ site}} - \text{entity value}_{Inj \text{ site}}}{\text{Sum of component lengths}} \right) = \left(\frac{e_{CS \text{ site}} - e_{Inj \text{ site}}}{\sum l} \right)$
17. The Ideal Gas Law, $PV = nRT$
18. Reservoir (rev) and Standard (std) States Analogy, $\left(\frac{PV}{zT} \right)_{res} = \left(\frac{PV}{T} \right)_{std} = \text{Constant}$
19. Darcy Radial Gas Flow, $Q_{std} = 858 \frac{K h (P_1^2 - P_2^2)}{\mu T \ln \frac{r_1}{r_2}}$
20. Interstitial Flow Throughput, $IFT = \frac{Q_{std}}{\phi} = 858 \frac{1 K h (P_1^2 - P_2^2)}{\phi \mu T \ln \left(\frac{r_{outer}}{r_{inner}} \right)}$
21. Number of Pores, $N_p = \frac{\phi \pi h (r_{outer}^2 - r_{inner}^2)}{\pi (r_{pore})^2 (r_{outer} - r_{inner})} = \phi h \frac{(r_{outer} + r_{inner})}{(r_{pore})^2}$
22. Interstitial Pore Holding Capacity, $IPHC = \frac{\text{Darcy Flowrate}}{\text{Number of Pores}} = \frac{Q_{std}}{N_p} = \frac{Q_{std} (r_{pore})^2}{\phi h (r_{outer} + r_{inner})}$
23. Reservoir Quality Index, $RQI = 0.0314 \sqrt{\frac{K}{\phi}}$

Experiments

The gas experiment used in this study is modelled according to previous authors' gas investigations, such as (Abunumah et al., 2021; Ogunlode et al., 2019). Structurally analogous core samples were selected for the experiments such that they bore a range of geological parameters (e.g., porosity, pore size, permeability, aspect ratio) found in reservoirs as reported in (al Adasani & Bai, 2011). The dimensional, geological, and morphological characteristics are shown in

Table 1, Table 2, and Figure 3, respectively.

The various characteristics significantly contribute to the flow mechanism (viscous flow, slip flow, Knudsen diffusion and surface diffusion) a fluid would experience in the pore matrix. The analogous core sample does not have the prerequisite organic components that enable surface diffusion flow mechanism. Thus, in this study, that flow mechanism was not considered. The CO₂ gas used was supplied by BOC. The core holder is made of stainless steel and the gas seals are granite seals. Figure 5 shows a schematic of the experimental setup and the

measuring devices used.

Table 1. The Five Core Samples and their Geometrical Characteristics

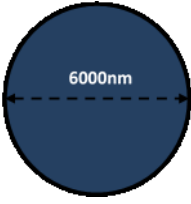
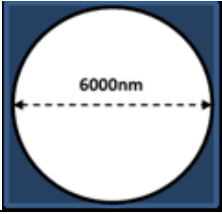
Media	Sample Code	Pore Diameter, nm	Porosity	Effective Permeate Length, cm	Radial Thickness, cm	Injection Area, cm ²	Media Volume, cm ³
	P13R15	15	13%	36.50	0.14	114	176
	P3R15	15	3%	65.10	0.25	524	3827
	P20R20	200	20%	36.60	0.15	124	224
	P14R6000	6000	14%	36.90	0.14	118	178
	P4R6000	6000	4%	37.10	0.24	300	2113

Table 2. Some Geological Characteristics of the Analogous Core Samples used in the Experiments

Sample Code	Total Pore Vol, cm ³	Unit Pore Vol, cm ³	Reservoir Quality Index, μm	Number of Pores	Aspect Ratio	Tortuosity
P13R15	7.29	2.0E-12	6.6E-03	3.6E+12	1.9E+05	3.38
P3R15	14.27	3.6E-12	1.4E-02	4.0E+12	3.4E+05	3.20
P20R20	13.19	3.9E-10	5.3E-03	3.4E+10	1.5E+04	3.49
P14R6000	7.76	3.1E-07	6.4E-03	2.5E+07	4.5E+02	3.42
P4R6000	10.47	5.5E-07	1.2E-02	1.9E+07	8.0E+02	3.84

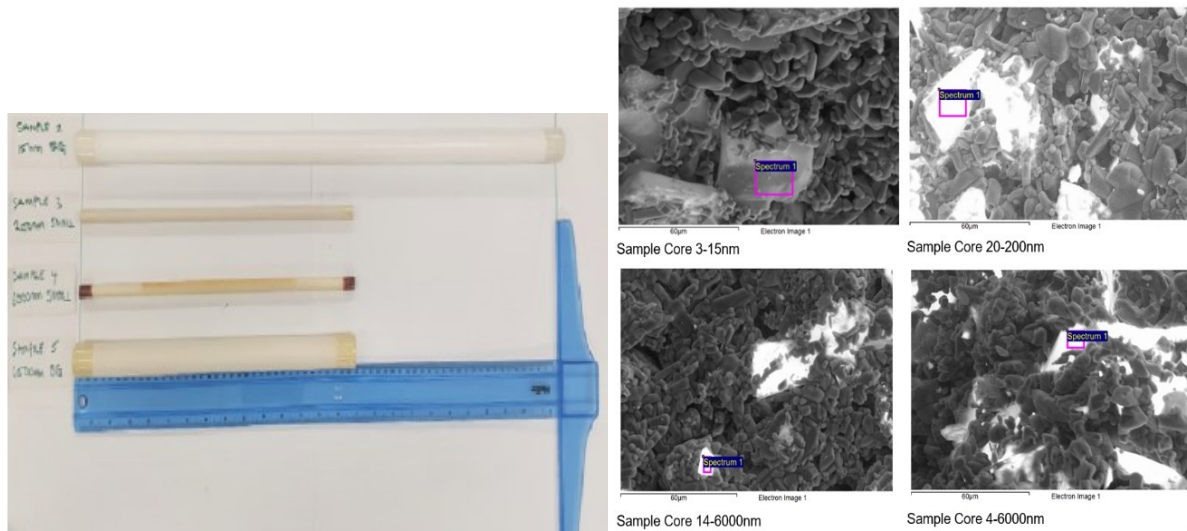


Figure 3. Four of the Analogous Core Samples and their SEM Morphologies

Experimental Procedure and Conditions

The experimental setup and equipment are shown in Figure 4. The core samples were placed inside a stainless steel core holder, and granite gas seals were placed on both ends of the sample before capping it with the core holder caps. A gas line with a pressure gauge was used to supply gas from the cylinder to the inlet of the core holder. A gas flow meter was connected to the core exit to receive the permeate. Three thermocouples and lagged heating tapes were wrapped around the core holder to regulate and measure the temperature of the system. The following procedure was carried out:

1. Heated and maintained the core system temperature to thermal stability (starting temperature: 293K).
2. Injected gas into the core system at a set pressure (starting pressure: 0.20 atm)
3. Record the permeate volume rate, temperature and pressure when the steady-state flow is achieved.
4. Steps 1-3 were repeated at intervals of 0.40 atm until the maximum pressure (3.0 atm) is reached.
5. Repeat a-d for temperatures 323, 373, and 432K.

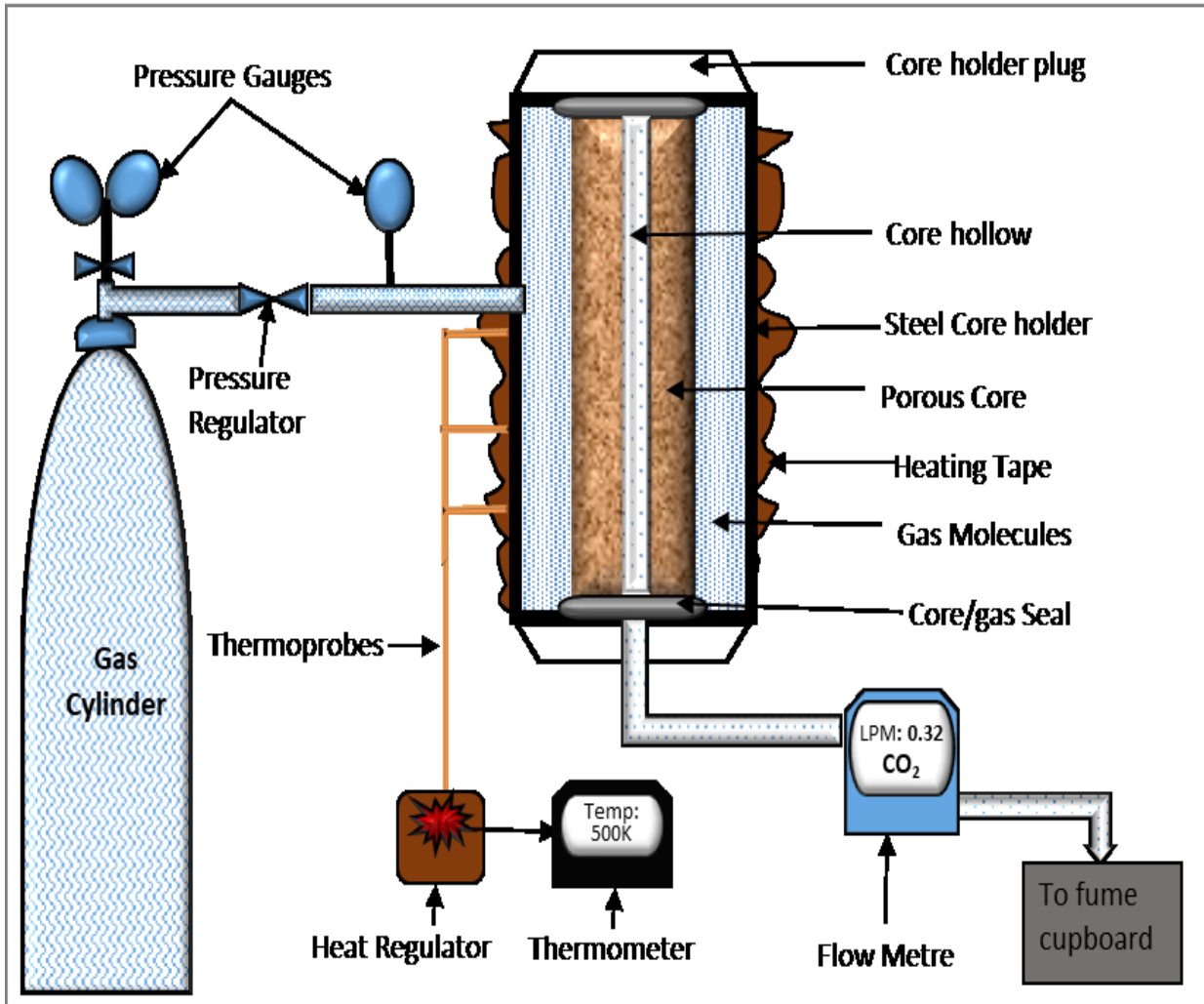


Figure 4. CO₂ Experimental Setup and Equipment used

Results

The CS analysis was conducted using the CO₂ flow profile in the respective analogous core samples. Figure 5 is a mother graph consisting of gas flow profiles at three isotherms (323K, 373K, and 423K). These temperatures are readily obtainable in geological reservoir settings for heavy oil, light oil and high-temperature and pressure (HTP) reservoirs, respectively (al Adasani & Bai, 2011). The juxtaposing of the isothermal flow enables the study to discover that CS response to reservoir structural parameters is affected by the core or reservoir temperature. It is generally observed that for all 5 samples and 3 isotherms, CO₂ effective permeation through pores are proportional to the pressure of the injected gas in each core sample. The relation can be aptly described by a power equation.

When the core samples temperature is at 323K, the magnitude of CO₂ flow throughput or permeations in P13R15, P3R15, P20R200, P14R6000 are similar and closely clustered. However, flow in P4R6000 is noticeably segregated from the other samples. This has implications in considering the CS potential of heavy oil reservoirs as they generally have temperatures that are less than 373K. At 373K (which is the average temperature of geological reservoirs), and 432K, CO₂ throughput in samples P4R6000 and P13R15 are segregated from the other samples. This implies that reservoir temperature above 373K can affect the CS potential of various structural layers of reservoir rocks. It is seen that at 373K and 423K, the P13R15 core sample allows the least CO₂ flow throughput at all operating pressure points. Therefore, suggesting that P13R15 offers a structural setting that relatively supports CS. Consequently, CSS engineers should consider reservoir layers with P13R15 type of structural setting as suitable sites for CO₂ deposition and sequestration.

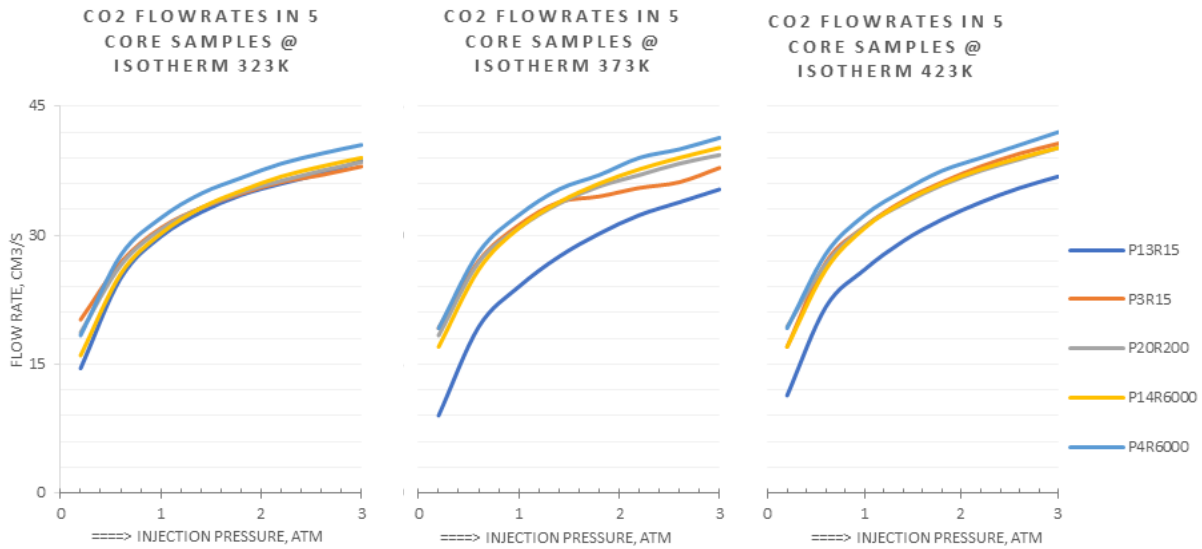


Figure 5. Flow Rate as a Measure of Evaluating CS Sites

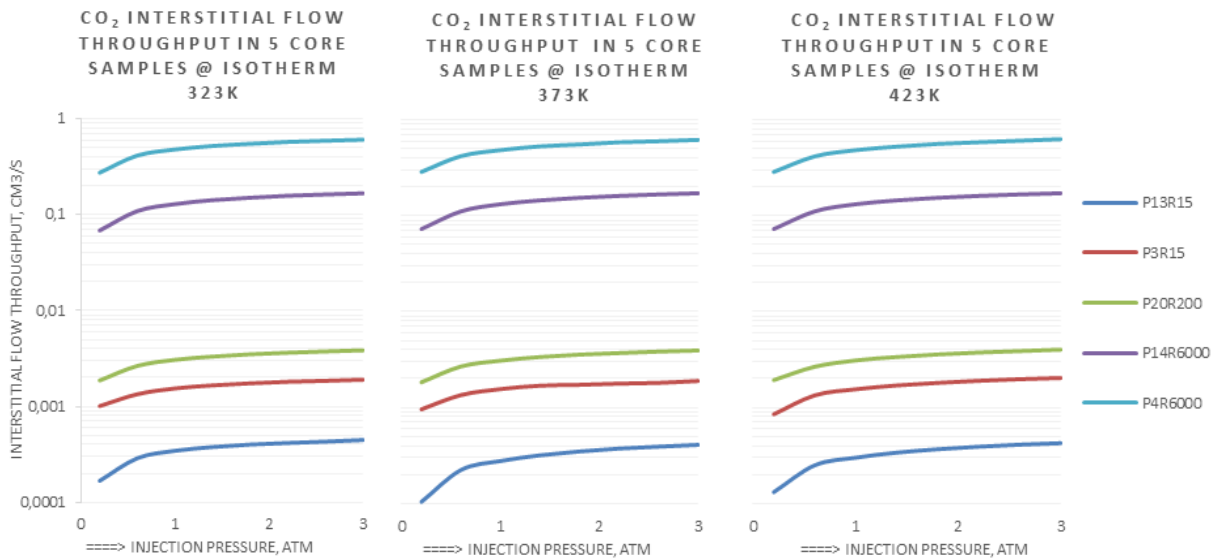


Figure 6. IFT for CO₂ in Five Core Samples at 3 Isotherms

The respective interstitial flow throughput (IFT) in the core samples is represented in Figure 6. This is obtained from the quotient of the Darcy flow rate and sample porosity. The IFT reflects the permeation behaviours of the CO₂ in the sample interstices as controlled or influenced by structural entities possessed by the interstices, such as tortuosity, porosity, aspect ratio and pore throat. Figure is a semi-log graph that shows the interstices flow throughput is quite segregated for all core samples. The core sample that allows the least IFT is P13R15. The characteristic of this sample can be understood and imposed on geological reservoirs.

The interstitial Pore holding capacity (IPHC) of porous media is a measure of the potential quantity of CO₂ molecules that can be distributed and held in the interstices and can be subsequently prevented from actively participating in flow throughput if the system is plugged or sealed. This is controlled by the effective pore volume-throat profile of the media and operating conditions of pressure and reservoir temperature. It has been previously stated that porosity (interstitial pore volume) controls the storage capacity of a media, while pore throat controls permeability or deliverability of fluids through the media (Grier, 1992). For CS optimisation, it is desired for IPHC to be maximised.

Consequently, in

Figure 7, P4R6000 and P14R6000 are respectively the samples with relatively high IPHC. This is could be due to their relatively large pore sizes of 6000nm and core radial thickness. It could be stated that the effect of porosity on IPHC in the different samples is negligible when the media pore size is relatively small as

demonstrated by the relatively close values of P3R15 and P13R15 when compared to P4R6000 and P14R6000. This finding to CCS implies that that reservoir layers with relatively large pore sizes offer better CS sites for CO₂ storage or holding capacity. Thereby it improves the reliability confidence of the CCS process.

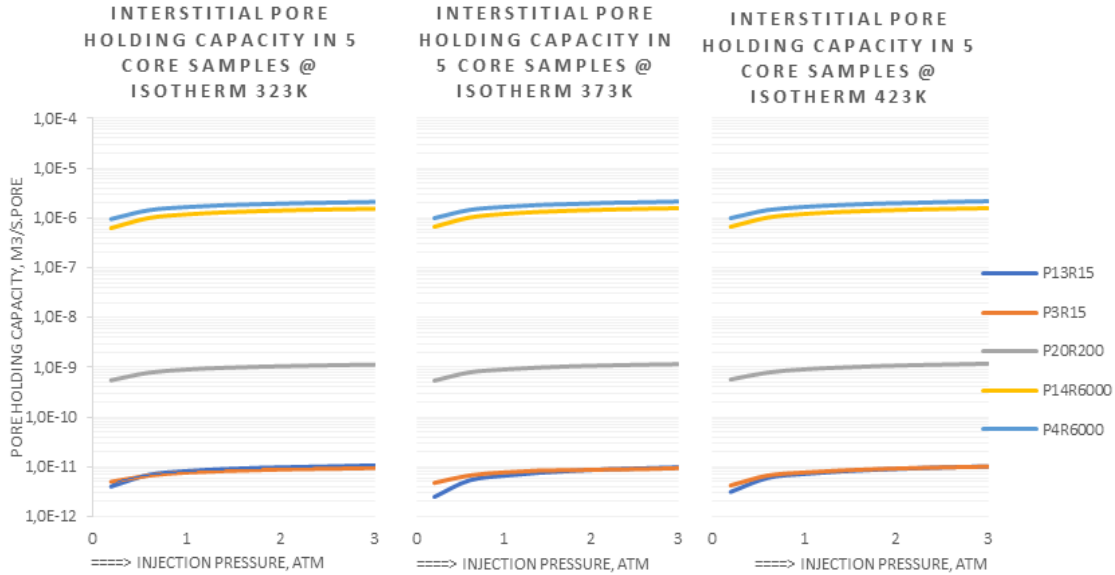


Figure 7. IPHC for the 5 Samples within Pressure Range 0.2-3.0atm

Discussion

The results above are discussed in the section in light of reservoir rhythm and gradient.

Rhythm

From the foregoing, the optimisation rhythm for CCS can thus be obtained for the two objective functions, Darcy flow and ITF. Table 3 shows the structural rhythm that optimises CS when Darcy flow was used as the optimisation criteria or objective function and minimum Darcy flow was used as the optimisation objective. It also shows the rhythm that supports maximum CO₂ sequestration and the placement of the CO₂ injection well. It is demonstrated that to optimise CS in multilayer reservoirs, the injection well should be located in the reservoir layer with characteristics similar to those of P4R6000.

Based on Table 23 description of analogous sample P4R6000, the reservoir layer should, therefore, comparatively possess the highest pore size, reservoir quality index and tortuosity; comparatively lowest porosity, number of pores, and aspect ratio. Similarly, the target CS site should be the layer that possesses characteristics analogous to core sample P13R15, which are, comparatively lowest pore size; comparatively higher porosity and aspect ratio; comparatively lowest reservoir quality index; comparatively highest pore numbers; and average tortuosity. This respective placement would ensure CS integrity.

Table 3. The Structural Rhythm that Optimises CS through Darcy Flow

Pore Dimension	Sample Code	Darcy Flow Rate, cm ³	Analogous Core Sample
Injection Site	P4R6000	34.25	A Suitable layer for Injection Well



Gradient

The gradient analysis was conducted to capture the reality of siting CO₂ injection wells relative to CS sites in reservoirs with geological layers that have different structural parametric values and compound rhythms. Optimisation requires that IFT should be as low as possible at the site where CO₂ is sequestered. Expectedly, IFT would be high at the site where CO₂ is injected into the compound layered system. Fifteen structural quantities have been investigated in

Table 4. It is shown that between the CO₂ injection and sequestration sites, CS optimisation requires 4 of the structural quantities to be positive gradients and 9 of them to be negative gradients. Porosity gradient for example is positive, this indicates that given a reservoir with multiple geological layers, for an effective CS, the injection well should be located such that it interfaces with the geological layer that has the highest porosity relative to the sequestration site. In contrast, the reservoir quality index (RQI) is required to be a negative gradient. Understandably so, because a low RQI in the sequestration site relative to the injection site means it would be difficult for CO₂ to permeate through or out of the CS zone. Thereby improving the integrity of the CS process.

Table 4. Structural Gradients that Facilitate CS Optimisation in Layered Reservoirs

**IFT optimisation requirements for CS:
High IFT (Injection site) → Low IFT (CS site)**

S/N	Structural Quantities	Gradient
1	Media/Layer Volume	-2092
2	Entering/Injection Area	-200
3	Void Volume	-3.43
4	Effective Permeate Length/Payzone	-0.65
5	Tortuosity	-0.50
6	CO ₂ Permeation per unit pay zone	-0.16

IFT optimisation requirements for CS: High IFT (Injection site) → Low IFT (CS site)		
S/N	Structural Quantities	Gradient
7	Radial Thickness	-0.11
8	Reservoir Quality Index	-0.01
9	Pore Size	-6.46E-04
10	Pore Holding Capacity	-1.93E-06
11	Unit Pore Volume	-5.89E-07
12	Porosity	0.10
13	Ln (r1 / r2) Or Reservoir-Wellbore Radia ratio	0.14
14	Aspect Ratio	2.05E+05
15	Number of Pores	3.89E+12

Conclusion

The study has thoroughly investigated CS from the perspective of taking advantage of natural reservoir structural rhythm and gradients. It has been concluded that not all reservoirs layer offers optimal CS to guarantee the reliability and integrity of the CCS process. It has been demonstrated that Darcy flowrate, IFT and IPHC can be used to characterise a layer's potential CS performance. The structural characteristics a potential CS site should possess has been presented and demonstrated. The major ones are that the site should bear the relatively lowest pore size; higher porosity and aspect ratio; relatively lowest reservoir quality index; relatively highest pore numbers; and average tortuosity. Furthermore, the structural gradients between the layers of the injection well and CS sites were found to be mostly negative gradients. Meaning, the magnitude or value of the considered structural quantity (such as pore size and tortuosity) at the CS site should be relatively lower than the quantity's magnitude or value at the injection point.

Recommendations

It is recommended that a two-phase experimental investigation be conducted to study how the presence of other reservoir fluids in the pores couple with the structural parameters to influence CS response to structural rhythm and gradients, and siting.

Acknowledgements

I would like to acknowledge the individuals and institutions that facilitated this research. This includes Prof Edward Gobina and the Doctoral Researchers at the Centre for Process Integration and Membrane Technology, Aberdeen, Robert Gordon University, Aberdeen, Ministry of Petroleum Resources, Abuja, Niger Delta Development Commission, Port Harcourt.

References

- Abunumah, O., Ogunlode, P., & Gobina, E. (2021). Experimental Evaluation of the Mobility Profile of Enhanced Oil Recovery Gases. *Advances in Chemical Engineering and Science*, 11(02), 154–164. <https://doi.org/10.4236/ACES.2021.112010>
- al Adasani, A., & Bai, B. (2011). Analysis of EOR projects and updated screening criteria. *Journal of Petroleum Science and Engineering*, 79(1–2), 10–24. <https://doi.org/10.1016/J.PETROL.2011.07.005>
- Anderson William White Wallace Broecker, D., Hayes, J., Hofmann, A., Holland Marcia McNutt Harry Elderfield Edward Stolper, H., Langmuir William McDonough Henry Shaw Richard, C. O., Hubert

- Staudigel, C., & Zindler, A. (1999). Climate change and greenhouse gases. *Wiley Online Library*, 80(39). <https://agupubs.onlinelibrary.wiley.com/doi/abs/10.1029/99EO00325>
- Andrei, M. M. A., & de Simoni, M. (2010). Enhanced Oil Recovery with CO₂ Capture and Sequestration. *World Energy Congress 2010 (WEC Montreal 2010)*, 2015–2034. <http://www.proceedings.com/08705.html>
- Crowley, T., Science, R. B., & 2001, undefined. (2001). CO₂ and climate change. *Science.ScienceMag.Org*, 292(5518), 870–872. <https://doi.org/10.1126/science.1061664>
- den Elzen, M. G. J., Olivier, J. G. J., Höhne, N., & Janssens-Maenhout, G. (2013). Countries' contributions to climate change: Effect of accounting for all greenhouse gases, recent trends, basic needs and technological progress. *Climatic Change*, 121(2), 397–412. <https://doi.org/10.1007/S10584-013-0865-6>
- Hertzberg, M., Siddons, A., & Schreuder, H. (2017). Role of greenhouse gases in climate change. *Energy and Environment*, 28(4), 530–539. <https://doi.org/10.1177/0958305X17706177>
- IPCC. (2018). *Summary for Policymakers of IPCC Special Report on Global Warming of 1.5°C approved by governments*. www.ipcc.ch
- Ledley, T. S., Sundquist, E. T., Schwartz, S. E., Hall, D. K., Fellows, J. D., & Killeen, T. L. (1999). Climate change and greenhouse gases. *Eos*, 80(39). <https://doi.org/10.1029/99EO00325>
- McGlade Christophe. (2019). *Can CO₂-EOR really provide carbon-negative oil?* - Google Scholar. https://scholar.google.com/scholar?hl=en&as_sdt=0%2C5&q=Can+CO2-EOR+really+provide+carbon-negative+oil%3F&btnG=
- Mintzer, I. M. (1990). Energy, greenhouse gases, and climate change. *Annual Review of Energy. Vol. 15*, 15, 513–550. <https://doi.org/10.1146/ANNUREV.EG.15.110190.002501>
- Neele, F., Quinquis, H., Read, A., Wright, M., Lorsche, J., & Poulussen, D. F. (2014). CO₂ Storage Development: Status of the Large European CCS Projects with EPR Funding. *Energy Procedia*, 63, 6053–6066. <https://doi.org/10.1016/J.EGYPRO.2014.11.638>
- Ogunlode, P., Abunumah, O., Orakwe, I., Shehu, H., Muhammad-Sukki, F., & Gobina, E. (2019). Comparative evaluation of the effect of pore size and temperature on gas transport in nano-structured ceramic membranes for biogas upgrading. *Rgu-Repository.Worktribe.Com*, 5, 195–205. <https://doi.org/10.32438/WPE.8319>
- Passalacqua, H., & Strack, K. (2020). *Reducing carbon footprint by geophysical monitoring of EOR processes*. 3384–3388. <https://doi.org/10.1190/SEGAM2020-3424907.1>
- S. P. Grier, D. M. M. (1992). *Reservoir Quality: Part 6. Geological Methods*. 95, 275–277. <http://archives.datapages.com/data/specpubs/methodo1/data/a095/a095/0001/0250/0275.htm>
- Saleh Aidrous Abdulla Al Wahedi, F., & Eddine Dadach, Z. (2013). *Cost Effective Strategies to Reduce CO₂ Emissions in the UAE: A Literature Review*. <https://doi.org/10.4172/2169-0316.1000116>
- Samset, B. H., Fuglestedt, J. S., & Lund, M. T. (2020). Delayed emergence of a global temperature response after emission mitigation. *Nature Communications*, 11(1). <https://doi.org/10.1038/S41467-020-17001-1>
- Shine, K. P., & Sturges, W. T. (2007). CO₂ is not the only gas. *Science*, 315(5820), 1804–1805. <https://doi.org/10.1126/SCIENCE.1141677>
- Verma, M. K. (2015). *Fundamentals of carbon dioxide-enhanced oil recovery (CO₂-EOR): A supporting document of the assessment methodology for hydrocarbon recovery using*. <https://doi.org/10.3133/ofr20151071>
- Wu, Z., & Liu, H. (2019). Investigation of hot-water flooding after steam injection to improve oil recovery in thin heavy-oil reservoir. *Journal of Petroleum Exploration and Production Technology*, 9(2), 1547–1554. <https://doi.org/10.1007/S13202-018-0568-7/FIGURES/10>